Published in final edited form as:
Cell Calcium. 2007 April ; 41(4): 397–403.

Modulation of local Ca^{2+} release sites by rapid fluid puffing in rat atrial myocytes

Sun-Hee Woo[1], **Tim Risius**[2], and **Martin Morad**[2,*]

1 *College of Pharmacy, Chungnam National University, 220 Gung-Dong, Daejeon, 305-764 Korea*

2 *Department of Pharmacology, Georgetown University Medical Center, 3900 Reservoir Road, NW, Washington DC, 20057 USA*

Abstract

Atrial myocytes that lack t-tubules, appear to have two functionally separate sarcoplasmic Ca^{2+} stores: a peripheral store associated with plasmalemmal L-type calcium channels and a central store with no apparent proximity to L-type calcium channels. Here we describe a set of calcium sparks and waves that are triggered by puffing of pressurized (200–400 mmH_2O) bathing solutions onto resting isolated rat atrial myocytes. Puffing of pressurized (200 mmH_2O) solutions, identical to those bathing the myocytes from distances of ~150 μm onto the surface of a single myocyte triggered or enhanced spontaneously occurring peripheral sparks by 5–6 fold and central Ca^{2+} sparks by 2–3 fold, without altering the unitary spark properties.. Exposure to higher pressure flows (400 mmH_2O) often triggered longitudinally spreading Ca^{2+} waves. These results suggest that pressurized flows may directly modulate Ca^{2+} signaling of atrial myocytes by activating the intracellular Ca^{2+} release sites.

1. Introduction

Contraction of mammalian cardiac myocytes is controlled by a sequence of events that is intiated by activation of L-type Ca^{2+} current (I_{Ca}) that in turn gates the Ca^{2+} release channels (ryanodine receptors, RyRs) of the sarcoplasmic reticulum (SR) [1–4]. Most of atrial myocytes have two functionally separate SRs: junctional SR close to the peripheral membrane and non-junctional or corbular SR confined to the central regions of the cell with no association to cell membrane, or the t-tubules, which are either absent [5,6] or partially developed [7–9]. Ca^{2+} release, initiated at the peripheral junctional sites by I_{Ca}, propagates into the interior of the cell partly by local diffusion of Ca^{2+} from the peripheral sites to more centrally located sites in atrial myocytes [10–14]. Such a compartmentation of SR may have evolved to mediate separate Ca^{2+} dependent functions: for instance, while junctional Ca^{2+} release may modulate membrane conductance via Ca^{2+}-dependent regulation of ion channels or transporters, such as K^+ channel, Cl^- channel and Na^+-Ca^{2+} exchanger [15,16], the central Ca^{2+} release is critical in activating the myofilaments.

Changes in the mechanical environment (volume and pressure) of the heart, caused by contractility of the heart, are known to alter cardiac excitation and contraction [17–19]. Pathological conditions, such as valve disease, hypertension or heart failure, may also lead to haemodynamic or mechanical dysfunction of the heart, causing arrhythmia [20–22]. Although

*Corresponding author: Martin Morad, Department of Pharmacology, Georgetown University Medical Center, 3900 Reservoir Road NW, Washington DC 20057, USA, Tel: +1 202 687 8440, Fax: +1 202 687 8453, Email: moradm@georgetown.edu

experimental evidence suggests that mechanical stress forces modulate intracellular Ca^{2+} signal in cardiac myocytes, there is significant controversy as to the effects of various modes of mechanical stimuli (e.g., stretch and shear stress) [23,24]. In this respect, in rat atrium, while electrically stimulated Ca^{2+} transients and contraction are enhanced by stretch with no change in the diastolic Ca^{2+} levels [25], direct fluid-induced shear stress seems to trigger transient increases in cytosolic Ca^{2+} [26].

The present study was designed to explore whether pressurized puff (PP) of bathing solutions affects local and focal Ca^{2+} signaling in the peripheral and central regions of atrial myocytes. PPs were applied to whole surface of myocytes through an electronically controlled microbarrel solution exchange system. This approach may approximate the mechanical stresses that the atrial chamber walls encounter from haemodynamic forces of flow (e.g., blood-jet to atrial wall during mitral regurgitation) or from excessive pressures produced during atrioventricular valve stenosis. Our data demonstrate that pressurized puffs of solutions generate longitudinal Ca^{2+} waves by triggering or increasing the frequency of occurrence of peripheral and central Ca^{2+} sparks.

2. Materials and methods

2.1. Single cell isolation

Rat atrial myocytes were enzymatically isolated from male Wistar WKY rats (200~300 g) as described previously [14]. Briefly, rats were deeply anesthetized with sodium pentobarbital (150 mg/kg, *i.p.*), the chest cavity was opened and hearts were excised. This surgical procedure was carried out in accordance with university ethical guidelines. The excised hearts were retrogradely perfused at 7 ml/min through the aorta (at 36.5°C), first for 3 min with Ca^{2+}-free Tyrode solution composed of (in mM) 137 NaCl, 5.4 KCl, 10 HEPES, 1 $MgCl_2$, 10 glucose, pH 7.3, and then with Ca^{2+}-free Tyrode solution containing collagenase (1.4 mg/ml, Type 1, Roche) and protease (0.14 mg/ml, Type XIV, sigma) for 12 min, and finally with Tyrode solution containing 0.2 mM $CaCl_2$ for 8 min. The ventricles of the digested heart were then cut into several sections and subjected to gentle agitation to dissociate the cells. The freshly dissociated cells were stored at room temperature in Tyrode solution containing 0.2 mM $CaCl_2$.

2.2. Application of pressurized puffs of solutions to the single atrial myocytes

Myocytes were continuously superfused with the Tyrode solution containing 2 mM Ca^{2+}. Pressurized puffs of solutions were applied to the whole area of single myocyte through a microbarrel (internal diameter = 250 μm) the tip of which was placed at ≈150 μm from the cell and was connected to a fluid reservoir with a height of 200- or 400-mm. Electronically controllable solenoid valve was installed in the middle of tubing connecting the fluid reservoir to the microbarrel, the tip of which, touching the chamber bottom, was tilted to one side with an angle of 45°. This system generated a flow force (in dyne/cm^2; [27]) of 7.2 and 16.3 at 200- and 400-mm reservoir heights, respectively. The positioning of the microbarrel was performed under microscope (Axiovert TV135, Zeiss, Germany) using a micromanipulator.

2.3. Two-dimensional confocal Ca^{2+} imaging and image analysis

Cells were loaded with the Ca^{2+} indicator dye fluo-4 AM (3 μM, 40 min) at room temperature and were imaged using a Noran Odyssey XL 2-D laser scanning confocal microscopy system (Noran Instruments, Madison, WI, USA) attached to a Zeiss Axiovert TV135 inverted microscope fitted with a ×40 water-immersion objective lens (Zeiss 440052 C-Apochromat, NA 1.2). The excitation wavelength of the argon ion laser was set to 488 nm (Omnichrome), and fluorescence emission (>510 nm) was detected by a high-efficiency PMT (Hamamatsu, Middlesex, NJ, USA). The *y* direction was scanned at 30 Hz. The confocal slit, stretching in

the *x* direction, was set to values corresponding to a width of 0.6 μm in confocal plane of the objective. The measured point-spread-function of the confocal microscope was approximately a truncated cylinder 0.3 μm in radius and 0.8 μm in length. Data were acquired by the Intervision program in a workstation computer (IRIX-operating system, Indy, Silicon Graphics).

Images were analyzed using a custom-written PC computer program in Visual Basic 6.0 (Microsoft). Focal Ca^{2+} releases were identified by a computerized algorithm as previously described [28]. The focal Ca^{2+} releases that had one stationary center for their growth and decay were then subjected to 2-D Gaussian approximations in a restricted area (30 pixels × 30 pixels), which allowed routine measurements of the amplitude, width and equivalent area of sparks originating from the peripheral and central regions [28]. Absolute spark amplitude ($F_1/F_{r)}$ was estimated as the central increase in fluorescence (F_1) measured relative to the resting average fluorescence (F_r) of the quiescent area with no spark. The measurement of absolute spark amplitude [29] enabled us to avoid uncontrolled variations of background fluorescence (F_0) of sparky area and estimate the local increase in cytosolic Ca^{2+} concentration. We have routinely measured the quality of the fit by calculating the standard deviation (SD, root-mean-square) between the raw data and the fitted Gaussian distribution. We compared these SD values to an estimate of the noise (individual pixels as compared to the mean their 8 nearest neighbors) and found that they agree within ~20% in ~85% of analyzed sparks.

We assumed that the major part of cell image excluding both ends of the cell, recorded at 30 Hz (see Figure 1B), to be a square. Then, the area up to 1.5 μm immediately underneath the cell membrane was denoted as the peripheral domain (peripheral area = 2 × 1.5 μm × image length, μm). The remaining area, measured as a difference between the whole image area and the peripheral area was considered as center.

2.4. Statistical analysis

Statistical comparisons were carried out using Student's *t* test. Differences were considered to be statistically significant to a level of $P < 0.05$. Numerical results are given as means ± SEM. All experiments were carried out at room temperature (22–24°C).

3. Results

3.1. Effect of pressurized puffs of solution on subcellular Ca^{2+} signals

We first examined the possible differential effects of PP on spontaneously occurring Ca^{2+} sparks recorded either at the central (nonjunctional) or peripheral (junctional) domains of quiescent atrial myocytes. Imaging for extended periods at 30 Hz was used to monitor the major portions of the myocytes and to compensate for the scarcity of spontaneously occurring sparks. Application of PP (200 mmH_2O) to atrial myocytes elicited *local* Ca^{2+} transients both in the periphery and center of myocyte (Fig. 1A). The PP-induced *local* Ca^{2+} transients were recorded more often in the cell periphery than in cell center (Fig. 1A, compare green and red traces). In addition, immediately following the exposure of myocyte to PP, Ca^{2+} spark-like events were activated at distinct focal sites (Fig. 1Bb-c). Though PP significantly increased the background basal Ca^{2+} levels in the center of myocytes, it did not alter the magnitudes of the transient Ca^{2+} rises (Fig. 1Ac). In contrast, the focal Ca^{2+} signals in the cell periphery became more diffuse and larger (Fig. 1Ad and Bd). The PP-induced focal and local Ca^{2+} transients were often detected at specific local sites repetitively (Fig. 1C, traces 1 and 3). Such highly active sites were more prevalent in the periphery than in the center of myocyte.

To determine the effect of PP on focal Ca^{2+} signals in more detail we attempted to identify the focal release sites in the 2-D confocal Ca^{2+} images using center-minus-surround detection kernel (see Materials and methods; [28]). Figure 2A compares 2-D confocal Ca^{2+} fluorescence

images recorded in the absence and presence of PP (200 mmH_2O; duration: 1.5 s) in a representative rat atrial myocyte. Single Ca^{2+} sparks were normally seen at 2–3 sequential frames (33 frames/s). The average frequency of sparks (events/[10^3 μm^2s]) in the control condition was significantly higher in the cell periphery (12.5 ± 2.3) compared to the center (2.61 ± 1.52, $P < 0.01$, n = 12), consistent with our previous reports [28]. The occurrence of spontaneous Ca^{2+} sparks was significantly increased both in the periphery and center by the application of PP of solutions (compare panel B and C in Fig. 2). The mean frequency of peripheral sparks increased by ~6 fold as compared to ~3 fold effect on the central sparks (Fig. 2D). Thus the effects of PP was 2-fold larger in the cell periphery than in the center.

Individual 2-D spark images were quantified by a spatial Gaussian approximation [27]. Figure 3 compares the unitary properties of spontaneous central and peripheral Ca^{2+} sparks measured in the presence and absence of PP. The amplitude (F_1/F_r), the full-width at half maximal amplitude (FWHA) and the area (μm^2) of Ca^{2+} sparks in the periphery and center were not significantly changed by PP of solutions and were similar to those recorded at rest (Fig. 3).

3.2. Development of longitudinal Ca^{2+} wave by high PP of solutions

When higher fluid pressures were applied to atrial myocytes, global Ca^{2+} waves were constantly activated. Figure 4A shows a representative Ca^{2+} wave that developed by application of higher (400 mmH_2O) PP of solution. The global Ca^{2+} wave started from a focal Ca^{2+} release site in the periphery (Fig. 4A, third image), and consistently propagated in a longitudinal direction from its focal origin (Fig. 4A). The focal origin of Ca^{2+} waves was either at the end of the cell or its perinuclear region, and often at a site close to the cell membrane. The velocity of PP-induced longitudinal Ca^{2+} waves was calculated as a distance between its starting and ending points (1 and 2 in the image of Fig. 4B), divided by the difference (delay) of time-to-peaks of Ca^{2+} releases of the two sites. Mean velocity of PP-induced Ca^{2+} waves measured in 7 cells was 78.4 ± 14.1 μm/s.

4. Discussion

In the present study we show that rapid flow of pressurized solutions significantly increases the frequency of spontaneous Ca^{2+} spark in the periphery and center of atrial myocytes without changing the unitary properties of the single sparks. The effect of fluid pressure puffs on the frequency of spark occurrences was two times larger in the periphery of the myocytes than in its center (Fig. 2D), suggesting that a mechanical sensor in the cell periphery may transmit the fluid pressure force. Some what larger fluid puffing pressures generated longitudinal Ca^{2+} waves which appear to be triggered by Ca^{2+} sparks (Fig. 4A). Mechanically induced Ca^{2+} waves have been seen in heart tissue [24] and in skeletal muscle [30], but the origin of the initiating Ca^{2+} flux has not been established.

Since the unitary properties of individual sparks were not significantly altered by fluid pressure puffs, it is reasonable to assume that the gating kinetics of RyRs was unaltered by the mechanical forces generated by PPs. The flow induced shear and pressure forces may deform the surface and the shape of the myocytes which in turn could mechanically stimulate the junctional dyads in the close proximity of the surface membrane. Alternatively, Ca^{2+} sparks maybe triggered by an inward collapse of surface membrane leading to a decrease in the junctional volume causing an increase in the Ca^{2+} concentrations of dyadic microdomains sufficient to activate Ca^{2+}-induced Ca^{2+} release locally. This possibility is consistent with the larger effects of PP on the frequency of peripheral Ca^{2+} sparks. A similar effect has been reported to occurs in skeletal muscle fibers where mild hypertonic solutions elicit Ca^{2+} sparks and waves secondary to local increases of Ca^{2+} concentrations in the cytosol or SR as the cell volume decreases [31,32].

Although it is not as yet clear what specific signaling pathway is activated by PP signaling, it has been reported that similar PP-induced increases in global Ca^{2+} concentrations in quiescent or electrically paced rat atrial myocytes, loaded with fura-2 AM, were not significantly altered by blockers of either strech-activated or Ca^{2+} channels and Na^{+}-Ca^{2+} exchanger (diltiazem 10 μM, Ni^{2+} 5 mM, or Cd^{2+} 1 mM, and Gd^{3+} 100 μM and withdrawal of external Ca^{2+}), as well as compounds that modulate nitric oxide signaling, but were strongly suppressed by several pharmacological modulators of mitochondria [26,33]. Nevertheless the, specific mechanisms for the PP-induced local Ca^{2+} changes need further investigation.

It has been reported that ~18% constant stretch of rat ventricular myocytes enhances spontaneous spark frequency with no global wave generation [34]. This report is somewhat comparable to our observation on the increased spark frequency in atrial myocytes during PP of solutions. The absence of Ca^{2+} efflux mechanism within the depth of atrial myocyte (absence of t-tubules), unlike the ventricular myocytes, may be the underlying mechanism for the development of central Ca^{2+} waves following the higher occurrence of Ca^{2+} sparks, and is probably responsible for the observed increase in resting Ca^{2+} of atrial myocytes (Figs. 1 and 4).

Our finding on the effects of PP on the frequency of spontaneous sparks and basal Ca^{2+}, on the other hand, is somewhat disparate from the previous report that the stretch of atrial muscle by increasing intra-atrial pressure did not affect diastolic indo-1 fluorescence ratio [25]. The difference in the two sets of observations may be, in part, due to the distinct mode of stimuli (fluid pressure vs. stretch) or different experimental preparations with or without extracellular matrices (intact heart vs. isolated cell). It should be also noted that when epifluorescence of the heart muscle is used in estimation of the intracellular Ca^{2+} of the mycoytes, part of the fluorescence signal may originate from cells other than myocytes, forming a possible source of error and low spatial resolution [35].

In the intact hearts it has been previously reported that an increase in the intra-atrial pressure with pressurized flow induces atrial fibrillation, and sustained arrhythmias [22]. The production of Ca^{2+} spark-mediated global Ca^{2+} wave by fluid pressure puffs, reported here, may in part underlie the cellular basis for the reported atrial fibrillation during the excessive intra-atrial pressure. We suggest that fluid pressure-induced Ca^{2+} releases may directly alter excitability of atrial myocytes by activation of intracellular Ca^{2+} pools that could in turn activate Ca^{2+}-dependent ionic conductance in the peripheral membrane. How fluid pressure is sensed and transmitted to the Ca^{2+} stores remains to be worked out.

Acknowledgements

This work was supported by NIH grant RO1-16125 to M. M. and the Korea Research Foundation grant funded by the Korean Government (MOEHRD) (KRF-2004-041-E00017) to S. -H. W.

References

1. Beuckelmann DJ, Wier WG. Mechanism of release of calcium from sarcoplasmic reticulum of guinea-pig cardiac cell. J Physiol 1988;405:233–255. [PubMed: 2475607]
2. Näbauer M, Callewaert G, Cleemann L, Morad M. Regulation of calcium release is gated by calcium current, not gating charge, in cardiac myocytes. Science 1989;244:800–803. [PubMed: 2543067]
3. Niggli E, Lederer WJ. Voltage-independent calcium release in heart muscle. Science 1990;250:565–568. [PubMed: 2173135]
4. Cleemann L, Morad M. Role of Ca^{2+} channel in cardiac excitation-contraction coupling in the rat: evidence from Ca^{2+} transients and contraction. J Physiol 1991;432:283–312. [PubMed: 1653321]

5. Sommer, JR.; Jennings, RB. Ultrastructure of cardiac muscle. In: Fozzard, HA.; Harbor, E.; Jennings, RB.; Katz, AM.; Morgan, HE., editors. The Heart and Cardiovascular System. New York: Ravan Press; 1992. p. 3-50.
6. Carl LS, Felix K, Caswell AH, Brandt NR, Ball WJ, Vaghy PL, Meissner G, Ferguson DG. Immunolocalization of sarcolemmal dihydropyridine receptor and sarcoplasmic reticular tridin and ryanodine receptor in rabbit ventricle and atrium. J Cell Biol 1995;129:673–682.
7. Forssmann WG, Girardier L. A study of the T system in rat heart. J Cell Biol 1970;44:1–19. [PubMed: 4901374]
8. Kirk MM, Izu LT, Chen-Izu Y, McCulle SL, Wier WG, Balke CW, Shorofsky SR. Role of the transverse-axial tubule system in generating calcium sparks and calcium transients in rat atrial myocytes. J Physiol 2003;547:441–451. [PubMed: 12562899]
9. Woo SH, Cleemann L, Morad M. Diversity of atrial local Ca^{2+} signaling: evidence from 2-D confocal imaging in Ca^{2+} buffered rat atrial myocytes. J Physiol 2005;567:905–921. [PubMed: 16020459]
10. Berlin JR. Spatiotemporal changes of Ca^{2+} during electrically evoked contractions in atrial and ventricular cells. Am J Physiol 1995;267:H1165–H1170. [PubMed: 7573513]
11. Hüser J, Lipsius SL, Blatter LA. Calcium gradients during excitation-contraction coupling in cat atrial myocytes. J Physiol 1996;494:641–651. [PubMed: 8865063]
12. Mackenzie L, Bootman MD, Berridge MJ, Lipp P. Predetermined recruitment of calcium release sites underlies excitation-contraction coupling in rat atrial myocytes. J Physiol 2001;530:417–429. [PubMed: 11158273]
13. Kockskämper J, Sheehan KA, Bare DJ, Lipsius SL, Mignery GA, Blatter LA. Activation and propagation of Ca^{2+} release during excitation-contraction coupling in atrial myocytes. Biophys J 2001;81:2590–2605. [PubMed: 11606273]
14. Woo SH, Cleemann L, Morad M. Ca^{2+} current-gated focal and local Ca^{2+} release in rat atrial myocytes: evidence from rapid 2-D confocal imaging. J Physiol 2002;543:439–453. [PubMed: 12205180]
15. Lipsius SL, Hüser J, Blatter LA. Intracellular Ca^{2+} release sparks atrial pacemaker activity. News Physiol Sci 2001;16:101–106. [PubMed: 11443225]
16. Mackenzie L, Bootman MD, Laine M, Berridge MJ, Thuring J, Holmes A, Li WH, Lipp P. The role of inositol 1,4,5-trisphosphate receptors in Ca^{2+} signaling and the generation of arrhythmias in rat atrial myocytes. J Physiol 2002;541:395–409. [PubMed: 12042347]
17. Lakatta EG. Cardiovascular regulatory mechanisms in advanced age. Physiol Rev 1993;73:413–467. [PubMed: 8475195]
18. Nazir SA, Lab MJ. Mechanoelectric feedback and atrial arrhythmias. Cardiovasc Res 1996;31:52–61. [PubMed: 8776403]
19. Kohl P, Hunter P, Noble D. Stretch-induced changes in heart rate and rhythm: clinical observations, experiments and mathematical models. Prog Biophys Mol Biol 1999;71:91–138. [PubMed: 10070213]
20. Copper G, Kent RL, Uboh CE, Thompson EW, Marino TA. Hemodynamic versus adrenergic control of cat right ventricular hypertrophy. J Clin Invest 1985;75:1403–1414. [PubMed: 3158672]
21. Komuro I, Kaida T, Shibazaki Y, Kurabayashi M, Katoh Y, Hoh E, Takaku F, Yazaki Y. Stretching cardiac myocytes stimulates protooncogene expression. J Biol Chem 1990;265:3595–3598. [PubMed: 2105950]
22. Bode F, Sachs F, Franz MR. Tarantula peptide inhibits atrial fibrillation. Nature 2001;409:14–15.
23. Calaghan SC, White E. The role of calcium in the response of cardiac muscle to stretch. Prog Biophys Mol Biol 1999;71:59–90. [PubMed: 10070212]
24. Sachs, F. Heart mechanoelectric transduction. In cardiac electrophysiology. In: Jalife, J.; Zipes, D., editors. From cell to bedside. Philadelphia: Saunders (Elsevier); 2004. p. 96-102.
25. Tavi P, Han C, Weckstrom M. Mechanisms of stretch-induced changes in $[Ca^{2+}]_i$ in rat atrial myocytes. Role of increased troponin C affinity and stretch-activated ion channels. Circ Res 1998;83:1165–1177. [PubMed: 9831710]
26. Morad M, Javaheri A, Risius T, Belmonte S. Multimodality of Ca^{2+} signaling in rat atrial myocytes. Ann N Y Acad Sci 2005;1047:112–121. [PubMed: 16093489]

27. Olesen SP, Clapham DE, Davies PF1. Haemodynamic shear stress activates a K^+ current in vascular endothelial cells. Nature 1988;331:168–170. [PubMed: 2448637]
28. Woo SH, Cleemann L, Morad M. Spatiotemporal characteristics of junctional and nonjunctional focal Ca^{2+} release in rat atrial myocytes. Circ Res 2003;92:e1–e11. [PubMed: 12522129]
29. Launikonis BS, Zhou J, Santiago D, Brum G, Rios E. The changes in Ca^{2+} sparks associated with measured modifications of intra-store Ca^{2+} concentration in skeletal muscle. J Gen Physiol 2006;128:45–54. [PubMed: 16769796]
30. Snowdowne KW. The effects of stretch on sarcoplasmic free calcium of frog skeletal muscle at rest. Biochim Biophys Acta 1986;862:441–444. [PubMed: 3778902]
31. Chawla S, Skepper JN, Hockaday AR, Huang CL. Calcium waves induced by hypertonic solutions in intact frog skeletal muscle fibres. J Physiol 2001;536:351–359. [PubMed: 11600671]
32. Martin CA, Petousi N, Chawla S, Hockaday AR, Burgess AJ, Fraser JA, Huang CL, Skepper JN. The effect of extracellular tonicity on the anatomy of triad complexes in amphibian skeletal muscle. J Muscle Res Cell Motil 2003;24:407–415. [PubMed: 14677643]
33. Belmonte S, Morad M. Accessing the mitochondrial regulation of puff-triggered Ca^{2+} transients in rat atrial myocytes. Biophys J 2006:521a.(Abstract)
34. Vila Petroff MG, Kim SH, Pepe S, Dessy C, Marbán E, Balligand JL, Sollott SJ. Endogenous nitric oxide mechanisms mediate the stretch dependence of Ca^{2+} release in cardiomyocytes. Nature Cell Biol 2001;3:867–873. [PubMed: 11584267]
35. Shinozaki T, Ishide N, Miura M, Takishima T. The source of epifluorescence in isolated perfused heart loaded with fura 2-AM or Indo-1 AM. Heart Vessels 1993;8:79–84. [PubMed: 8314741]

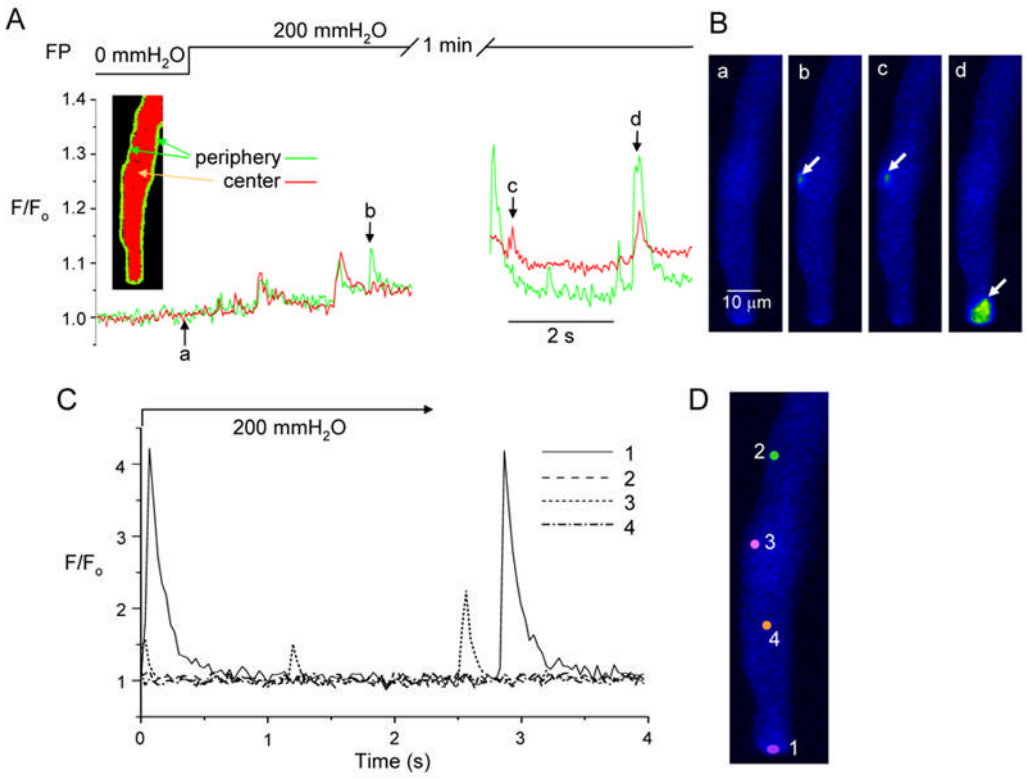

Fig 1.

Pressure puffing (PP)-induced local and focal Ca^{2+} release in rat atrial myocytes. (A) Effect of FP (200 mmH_2O) on time courses of local Ca^{2+} signals (30 Hz) measured in the periphery and center of fluo-4 AM loaded myocytes. Same extracellular solution was applied continuously for 2 min using pressurized puffing apparatus. Inset image show pixel masks to measure Ca^{2+} signal from the cell periphery (green) and center (red). (B) 2-D confocal Ca^{2+} images, measured at the time points indicated by a, b, c and d in the panel A. Color scale for fluorescence intensity is shown in the Fig. 4A. (C) Repetitive focal Ca^{2+} releases from the same local sites during PP (see traces *1* and *3*). The numbered Ca^{2+} signals (*1–4*) were measured from the subcellular sites indicated by the corresponding numbers in panel D. (D) Map of the locations of focal sites where the Ca^{2+} signals in panel C were measured.

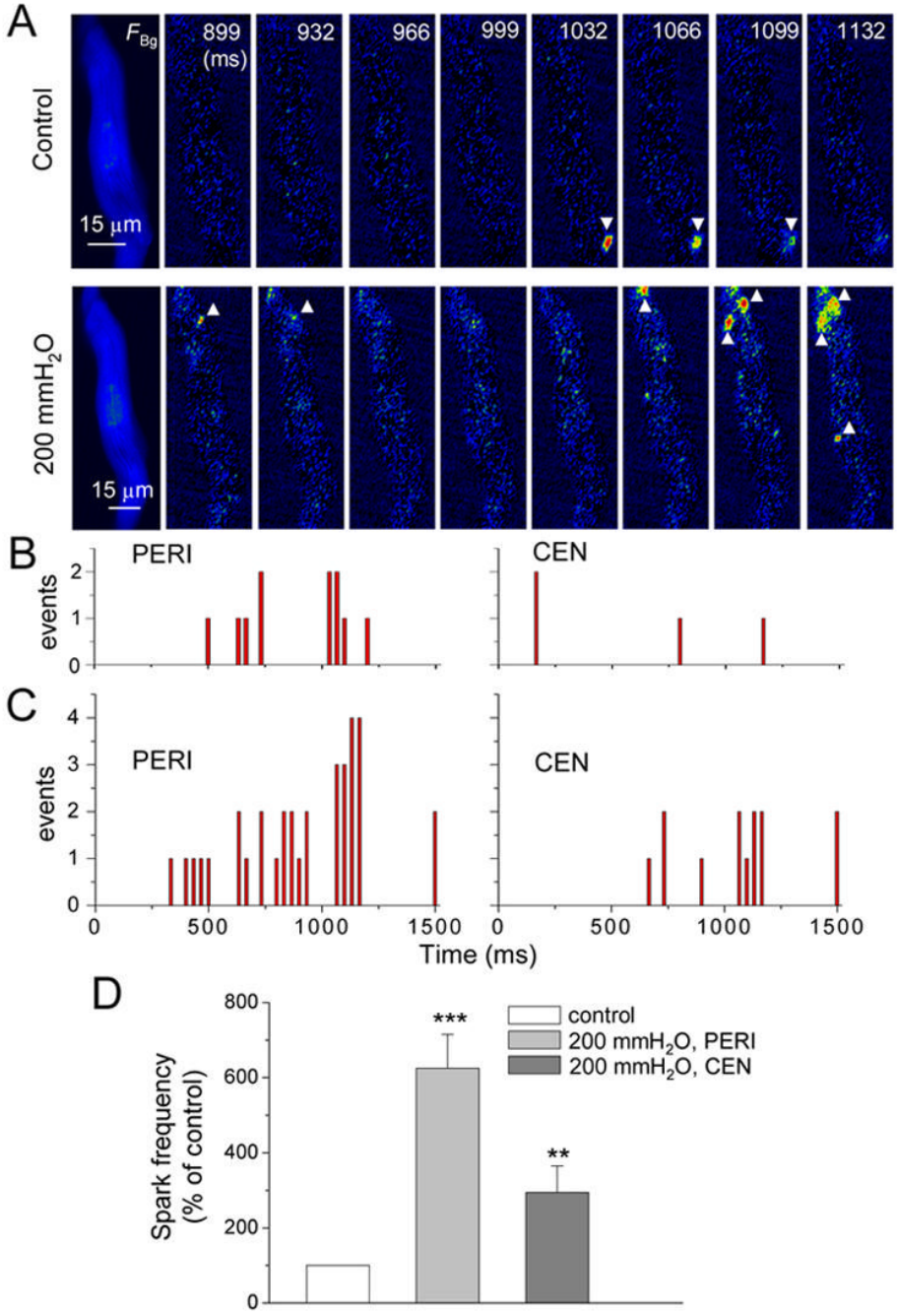

Fig 2.

Enhancement of spontaneous Ca^{2+} sparks by PP. (A) Sequential 2-D confocal Ca^{2+} images measured at 30 Hz during periods indicated by the numbers on top of each image. Upper and lower images were obtained before (control) and after applying PP (200 mmH_2O). Image F_{Bg} shows average fluorescence, revealing the clear outline of the myocytes. Numbered images, 899 to 1132 ms, are sequential frames measured differentially as the increase in fluorescence (ΔF) relative to the average fluorescence. In the differential measurements of fluorescence, the outline of the cell is seen as only variations in the noise, but Ca^{2+} sparks appear clearly (arrowheads). (B and C) Right and left panels show time courses of the occurrences of peripheral (PERI) and central (CEN) sparks in cell shown partly in panel A

before (B) and after (C) application of FP. (D) Mean increase in the frequency of central and peripheral Ca^{2+} sparks by FP (200 mmH_2O) compared to the control condition. ***P<0.001 vs. peripheral spark frequency in the control condition. **P<0.01 vs. central spark frequency in the control condition (n = 12).

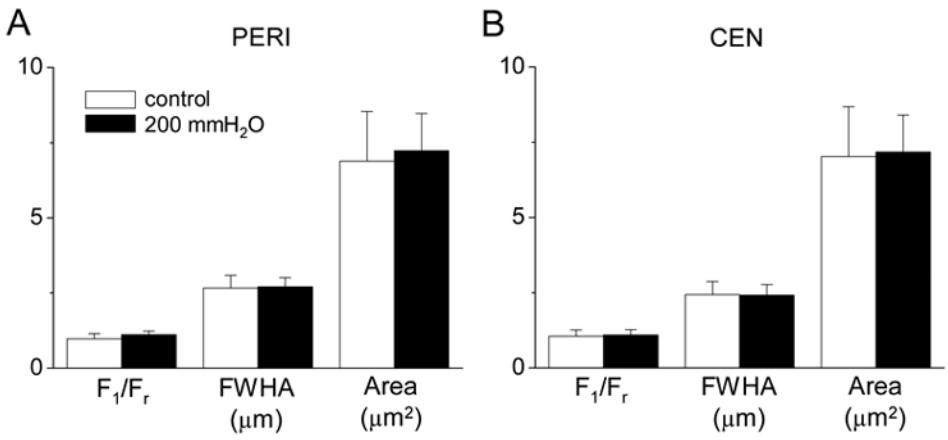

Fig 3.

Effect of PP on the unitary properties of Ca^{2+} sparks. Comparison of means of amplitude (F_1/F_r), full-width at half maximal amplitude (FWHA) and area of single peripheral (A, PERI: control, n = 41; PP, n = 210) and central (B, CEN: control, n = 73, FP, n = 196) sparks in the presence and absence of PP (200 mmH_2O; 12 cells). *P* values were >0.05 in the comparisons of all three parameters between control and PP. For detail see Materials and methods.

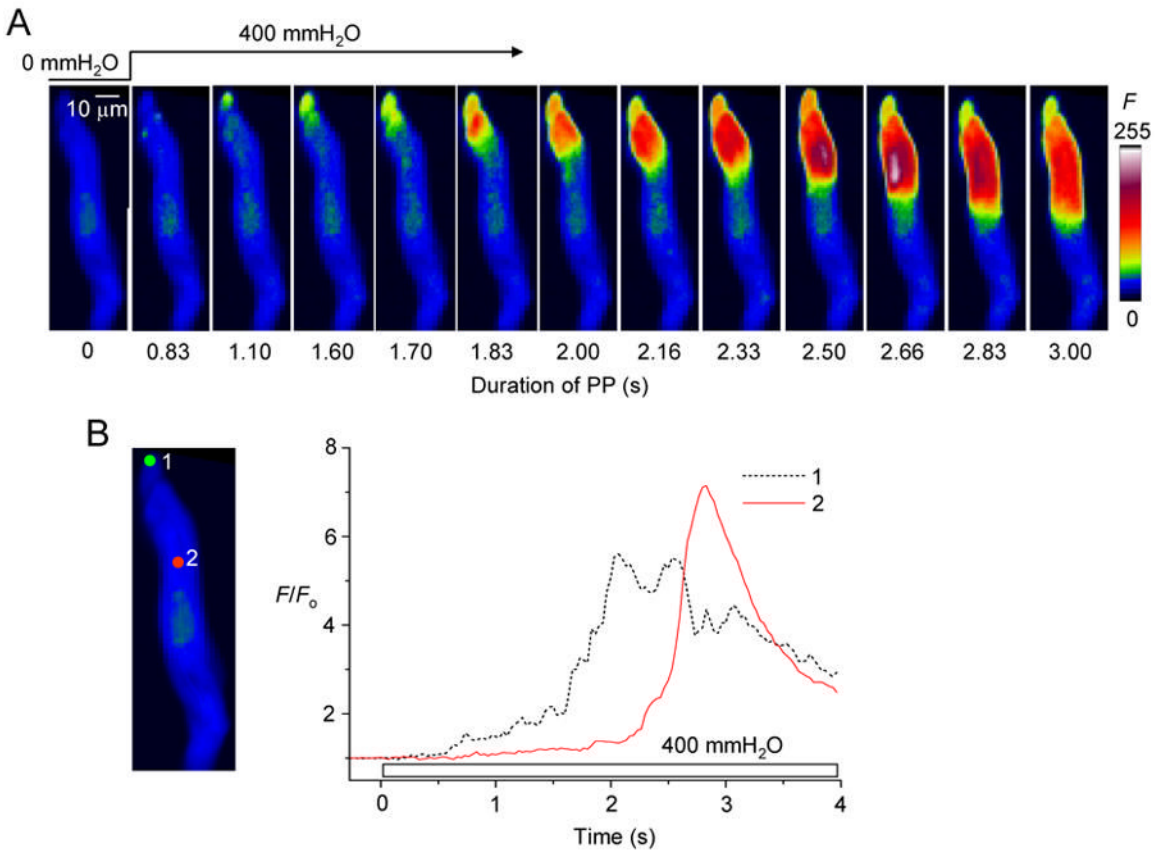

Fig 4.

Higher PP-induced longitudinal Ca^{2+} wave. (A) 2-D confocal Ca^{2+} images, recorded at the indicated times (see below each image) following application of FP of 400 mmH_2O, show development of a longitudinal Ca^{2+} wave by PP. (B) Ca^{2+} fluorescence signals (1 and 2) measured from the corresponding local sites, "1 (green)" and "2 (red)", in the left confocal image. Imaging was performed at 30 Hz.